Pediatric Radiology (2018) 48:1364–1375
https://doi.org/10.1007/s00247-018-4113-0

PEDIATRIC BODY MRI

Imaging of cancer predisposition syndromes

Mary-Louise C. Greer[1]

Received: 21 October 2017 / Revised: 28 January 2018 / Accepted: 11 March 2018

Abstract
Pediatric cancer predisposition syndromes comprise a group of diseases characterized by specific tumors or a concomitance of tumors in infants, children and adolescents, suggesting a genetic cancer susceptibility condition. Most but not all have germline pathogenic variants on genetic testing. For some children with cancer predisposition syndromes, this diagnosis is based on their own or a family history of related neoplasms, or associated clinical manifestations. These tumors have variable incidence and age of onset. Imaging encompasses investigation in symptomatic children for diagnosis, staging and monitoring for treatment response and metastatic disease, as well as surveillance for primary tumors in asymptomatic children. In this review the author focuses on the role of surveillance imaging in childhood cancer predisposition syndromes, whole-body magnetic resonance imaging (whole-body MRI) in particular. Diagnosis and staging of specific tumors are addressed elsewhere in this series. The benefits of surveillance imaging include early detection and improved outcomes and are still being established for a number of cancer predisposition syndromes. The benefits must be weighed against risks including potential technique-related issues relating to sedation or contrast agents, false-positive imaging findings, and cost — both financial and psychosocial. The author discusses general principles for whole-body MRI interpretation along with findings in specific syndromes where whole-body MRI screening is recommended, such as Li–Fraumeni syndrome.

Keywords Cancer predisposition syndrome · Children · Genetics · Li–Fraumeni syndrome · Oncology · Surveillance · Whole-body magnetic resonance imaging

Introduction

Cancer predisposition syndromes comprise a group of diseases characterized by specific tumors or a concomitance of tumors, benign and malignant, suggesting a genetic cancer susceptibility condition [1]. These can manifest from infancy to adulthood and are often of unknown penetrance, variable incidence, and differing age of onset of a range of neoplasms [2]. Most children with cancer predisposition syndromes are confirmed to have underlying germline pathogenic variants [3, 4]. Imaging in these children can be initiated (1) to evaluate a tumor presenting clinically; (2) when a pathogenic germline variant is detected on genetic testing, typically after diagnosis of a cancer predisposition syndrome-related tumor in another family member; or (3) when a child meets clinical criteria suggesting surveillance is warranted [4–6].

In symptomatic children, imaging encompasses initial diagnostic assessment and staging, with subsequent monitoring for treatment response, local recurrence or distant disease. These are addressed elsewhere in this series. Surveillance often incorporates physical examination, laboratory testing and imaging investigations. Integration of imaging for surveillance with the diagnostic imaging pathway is necessary to avoid duplication [6]. Alternatively, surveillance imaging can occur independently in asymptomatic children.

This review centers on surveillance imaging in pediatric cancer predisposition syndromes, including current recommendations for whom to screen, the particular role of whole-body MRI, and syndromes in which whole-body MRI is considered justified, recognizing that the evidence might be limited.

✉ Mary-Louise C. Greer
mary-louise.greer@sickkids.ca

[1] Department of Diagnostic Imaging, The Hospital for Sick Children, Department of Medical Imaging, University of Toronto, 555 University Ave., Toronto, ON M5G 1X8, Canada

Surveillance imaging

As our knowledge of the spectrum of pathology resulting from germline mutations increases, so too do the challenges of balancing early disease detection and improved outcomes against the risk of investigation. This is never more so than in children with an increased risk of cancer. The first step in achieving this balance is to determine whom to screen. In addition to pediatric patients confirmed to have a cancer predisposition syndrome based on a germline mutation, surveillance is also advocated if: (1) there is a family history of the same or a related tumor; (2) tumors are bilateral, multifocal or multiple; (3) tumors occur at an earlier age than sporadic tumors; (4) there are physical findings of a cancer predisposition syndrome such as macroglossia in Beckwith–Wiedemann syndrome or café-au-lait macules in neurofibromatosis; or (5) the child has specific cancer predisposition-syndrome-related tumors, such adrenocortical carcinoma in Li–Fraumeni syndrome or pleuropulmonary blastoma in *DICER1* syndrome [2, 4, 5].

The benefits of surveillance imaging in childhood cancer predisposition syndromes are substantiated in only a small number to date, such as in Li–Fraumeni and Beckwith–Wiedemann syndromes and in a preliminary study of hereditary retinoblastoma survivors [7–10]. However at least 8.5% of childhood malignancies are now thought to have an underlying genetic association, and as such the potential benefits of screening are likely even greater than is understood [11]. For this reason, Brodeur et al. [12] proposed surveillance in childhood cancer predisposition syndrome when the risk of developing a neoplasm is greater than 5% in the first two decades and 1–5% in select cancers that are rapidly progressive and aggressive, such as rhabdoid tumors [13]. The American Academy for Cancer Research (AACR) Pediatric Working Group recently published a series of cancer predisposition syndrome surveillance recommendations, developed by the consensus of a group of international experts from pediatric oncology, genetics, endocrinology and radiology [12]. These incorporated existing guidelines as available, some with modification, and created new recommendations where none existed. These surveillance recommendations include clinical evaluation, laboratory tests and imaging investigations for more than 50 childhood cancer predisposition syndromes.

Because of the ionizing radiation-sensitivity of pediatric patients, most surveillance imaging protocols rely more on ultrasound and MRI than nuclear medicine or computed tomography (CT), as appropriate to the tumor site being evaluated [14–16]. This is of particular importance in children with Li–Fraumeni syndrome, who have higher risks from ionizing radiation [17]. In a recent prospective study of people with Li–Fraumeni syndrome [8], those undergoing surveillance had statistically significantly longer survival times than those who did not. Whole-body MRI contributed most to the detection of malignancy in these patients, although it identified only 30% of malignancies, with overall outcomes achieved through utilization of all elements of the surveillance protocol. These included dedicated brain MRI, mammography, abdominal and pelvic ultrasound, blood work and clinical examination [8]. Recognizing the expanding role of whole-body MRI in the childhood cancer predisposition syndrome population, a subset of syndromes has been identified by the AACR Pediatric Working Group in which whole-body MRI surveillance is most beneficial; this subset is further delineated here, emphasizing "core" lesions [6, 12, 18].

Whole-body MRI surveillance imaging

Whole-body MRI, with its exquisite soft-tissue contrast and high spatial resolution, large field of view and lack of ionizing radiation, is well suited to demonstrate potentially multifocal disease seen in cancer predisposition syndromes. It can be complemented by targeted small field-of-view imaging for problem-solving and supplemented with dedicated regional studies such as brain MRI in Li–Fraumeni syndrome. Sensitivity remains low for lung nodules and lymph nodes less than 6 mm, with MRI not yet standard for lung surveillance [19]. On review of recently published whole-body MRI protocols for pediatric oncology, coronal short-tau inversion recovery (STIR) and axial half-Fourier single-shot turbo spin echo (HASTE) sequences are most commonly employed, with diffusion-weighted imaging (DWI) being a more recent addition [6]. Coverage is usually from vertex to heels, with separately acquired stations merged and displayed as whole-body fused coronal images for STIR and DWI, as well as sagittal imaging, although this is less commonly acquired. Further detail regarding whole-body MRI technique can be found in separate publications [19–21].

Utilization of whole-body MRI in pediatric cancer predisposition syndrome surveillance was first highlighted in 2011 by Monsalve et al. [2], who advocated annual whole-body MRI be performed in Li–Fraumeni syndrome for rhabdomyosarcoma and osteosarcoma. This group also summarized key cancer predisposition-syndrome-related tumors seen in a range of syndromes. Building on this knowledge by applying a systematic approach to whole-body MRI interpretation, with careful analysis of the at-risk anatomical sites, can optimize image analysis with the goal of improving lesion detection while minimizing false-positive findings [6, 18, 21]. Lecouvet [21] described a step-wise approach to whole-body MRI interpretation in oncology, including initial review of source or "native" images before analyzing the merged images, and through simultaneous comparison of the different sequences employed. An anatomical checklist by Greer et al. [6] in the AACR series further promotes a systematic approach to whole-body MRI interpretation in childhood cancer predisposition syndromes.

In a 2015 study by Anupindi et al. [18, 22], whole-body MRI was shown to have high sensitivity and negative predictive value of 100%, with a specificity of 94% and positive predictive value of 25%, on review of 50 whole-body MRIs in 24 pediatric patients with cancer predisposition syndromes. Most commonly performed for hereditary pheochromocytoma and paraganglioma syndromes and Li–Fraumeni syndrome, abnormalities were seen in 18% of whole-body MRIs, with a confirmed malignancy in 2%. This compares with 4.6% of cancer predisposition syndrome-related malignancies reported on 132 whole-body MRIs in 47 patients in another pediatric cohort [23]. Anupindi et al. [18, 22] also emphasized that false-positive findings can be a potential risk in whole-body MRI surveillance of cancer predisposition syndromes, warranting expert interpretation for optimal risk stratification. This is particularly important if incidental or nonspecific findings trigger further imaging with ionizing radiation or invasive testing [6, 18]. Additional potential risks relate to MRI technique — with typical need for general anesthesia in children younger than 6 years at the author's institution — and intravenous gadolinium-based contrast agents, although contrast agent is infrequently used in whole-body MRI for surveillance imaging [15, 16, 24, 25].

Another consideration in weighing risk versus benefit in surveillance imaging is cost. This can be considered in terms of the financial cost, time and psychosocial impact, with genetic counseling integral to patient recruitment for surveillance [4]. In addition to harmonizing surveillance and diagnostic imaging pathways, as previously stated, consideration of imaging frequency and scheduling — when to start and stop — is of equal importance and should be based on tumor pathophysiology, with examples given for specific cancer predisposition syndromes reviewed here [12].

Whole-body MRI in specific cancer predisposition syndromes

The AACR Pediatric Working Group has recommended whole-body MRI surveillance for the following childhood cancer predisposition syndromes: Li–Fraumeni syndrome, neurofibromatosis type 1, neurofibromatosis type 2 and schwannomatosis, hereditary retinoblastoma, constitutional mismatch repair deficiency syndrome and hereditary paraganglioma pheochromocytoma syndrome [6, 17, 26–30]. For a few additional syndromes — namely *DICER1* syndrome, rhabdoid tumor predisposition syndromes and Rothmund–Thomson syndrome — use of whole-body MRI is considered optional [6, 13, 31, 32]. In *DICER1* syndrome, other modalities provide suitable alternatives based on lesion location, with ultrasound for detecting ovarian or renal lesions, and chest radiography alternating with CT for pleuropulmonary blastomas [3, 14, 31]. In rhabdoid tumor predisposition syndrome type 1, *SMARCB1* carriers have an increased incidence of a range of tumors in addition to rhabdoid tumors, including schwannomatosis and malignant peripheral nerve sheath tumors. Although Foulkes et al. [13] suggested whole-body MRI might have a role, they added that utility is in question, with few data existing to guide timing and frequency. Type 2 Rothmund–Thomson syndrome has an increased risk of osteosarcoma; however is autosomal-recessive and its extreme rarity places doubt on the value of screening, whether with X-rays or MRI [32, 33]. The childhood cancer predisposition syndromes for which whole-body MRI is advocated by the AACR are reviewed next, including the relevant germline pathogenic variant; inheritance, prevalence and incidence where known; tumor spectrum and site; and imaging recommendations.

Li–Fraumeni syndrome

Li–Fraumeni syndrome (Online Mendelian Inheritance in Man [OMIM] #151623) is a high-risk autosomal-dominant cancer predisposition syndrome characterized by early onset. This is the result of heterogeneous pathogenic germline *TP53* mutations on chromosome 17p13.1, 70–75% having a missense mutation in this tumor-suppressor gene, with rarer variants increasingly identified [2, 7, 17, 34]. A recent meta-analysis of baseline surveillance using whole-body MRI by Ballinger et al. [35] described a lifetime risk of almost 100% of developing one or more malignancies, with primary malignant lesion occurrence peaking in children and in older adults. While classically presenting with a sarcoma before 45 years of age, in a cohort of new primary malignancies in asymptomatic *TP53* mutation carriers detected on whole-body MRI, 31% of patients were younger than 18 years (range 2–17 years), and 16% were between 18 years and 40 years [35]. Brain and bone tumors were more common in childhood. Males and females were similarly affected [17, 35]. The overall incidence of new primary malignancies was 7%, which was higher when performing whole-body MRI screening for Li–Fraumeni syndrome than for a range of other cancer predisposition syndromes [18, 23, 35]. Prevalence estimates vary widely because of ascertainment bias, ranging from 15% to 50% in people younger than 30 years [17, 36].

Core cancers in Li–Fraumeni syndrome are osteosarcoma, adrenocortical carcinomas, brain tumors, soft-tissue sarcomas and premenopausal breast cancer [2, 17]. In a prospective study by Villani et al. [8], the following heterogeneous tumor spectrum was identified: benign tumors included thyroid adenoma, breast fibroadenoma and meningioma; premalignant or low-grade neoplasms included myelodysplastic syndrome, osteochondroma, ductal carcinoma-in-situ, low-grade glioma, dysplastic nevus, melanoma-in-situ, squamous cell carcinoma and thyroid Hürthle cell adenoma; and malignant tumors included malignant fibrous histiocytoma, osteosarcoma,

adrenocortical carcinoma, invasive ductal carcinoma, breast cancer, choroid plexus carcinoma, chordoma, ependymoma, colorectal carcinoma and lung carcinoma. The meta-analysis by Ballinger et al. [35] also included astrocytoma, papillary thyroid cancer and renal carcinoma. Thyroid and renal cancer and lung adenocarcinoma have a higher occurrence in young adults in Brazil, the result of a *TP53* founder effect mutation, which is also associated with higher incidence of childhood adrenocortical carcinomas (8% of total tumors versus 4% in classic Li–Fraumeni syndrome), prompting intensified neonatal screening, with later onset of adult tumors [17, 35].

To optimize lesion detection on whole-body MRI, the following anatomical locations should be closely interrogated in Li–Fraumeni syndrome: highest-risk sites include brain (warranting dedicated MRI), adrenals, breast, bone and soft tissues; lower-risk sites include bowel, bone marrow and skin; Brazilian founder mutation sites include thyroid, lungs and kidneys. As emphasized by Lecouvet [21], sites warranting particular review are vertebral bodies and posterior elements, ribs and skull; this is especially true in Li–Fraumeni syndrome where use of radiography and CT should be minimized (Fig. 1). The young onset and multiplicity of primary malignancies in Li–Fraumeni syndrome are highlighted by the patient in Fig. 2, already with a second primary malignancy at 3 years old, necessitating a high level of vigilance in surveillance imaging. However, if nonspecific, lesions can be further evaluated with limited targeted imaging at the time of a surveillance scan, dedicated regional imaging then or later, as well as follow-up whole-body MRI (Fig. 3). Whole-body MRI surveillance recommendations for childhood Li–Fraumeni syndrome and accompanying imaging studies, as recommended by the AACR group, are summarized in Box 1 [6, 17].

Box 1

Li–Fraumeni syndrome

- Whole-body MRI every 12 months from diagnosis
- Brain MRI every 12 months from diagnosis (non-contrast after first if negative)
- Brain MRI and whole-body MRI interleaved at 6-month intervals if no general anesthetic required
- Abdominal & pelvic ultrasound every 3–4 months

Hereditary paraganglioma and pheochromocytoma syndromes

Hereditary paraganglioma and pheochromocytoma syndromes are also autosomal-dominant and can arise from germline pathogenic mutations in *SDHx* genes or in an array of non-*SDHx* genes, e.g., *MAX* gene, with penetrance nearing 90% [29, 37]. Mostly benign, these tumors of neural crest cell origin include extra-adrenal and adrenal tumors, paragangliomas and pheochromocytomas, respectively. Detected from 6 years to 8 years old onward, they may manifest by hormonal effect — tumors derived from the sympathetic nervous system in the lower mediastinum, abdomen and pelvis being catecholamine-secreting, versus non-secreting parasympathetic nervous system tumors in the base of skull, neck and upper mediastinum; or by mass effect — with a size-dependent propensity to metastasize [29, 38]. Malignant transformation is more common in hereditary than sporadic germline pathogenic variants. Together with other tumors seen in hereditary pheochromocytoma and paraganglioma syndromes, they are known collectively as the *SDHx*-related tumors, although they can occur in other cancer predisposition syndromes, such as Von Hippel–Lindau syndrome [37, 39, 40]. Other *SDHx*-related tumors include gastrointestinal stromal tumors, which are often multifocal and gastric in origin; renal tumors including oncocytoma; renal cell carcinoma; and rarely pituitary adenomas [29, 37, 39, 40].

Whole-body MRI coverage in hereditary pheochromocytoma and paraganglioma syndromes can be limited to the neck and trunk — denoted by "NCAP whole-body MRI" (neck, chest, abdomen and pelvis) or "CAP whole-body MRI" (chest, abdomen and pelvis) as suggested by Greer et al. [6]. Whole-body MRI has been shown to be more sensitive than biochemical testing (87.5% versus 37.5%) with comparable specificity (94.7% versus 94.9%) [6, 29, 39]. Key anatomical sites for review are the adrenals; autonomic nervous system, including the sympathetic trunk in the paravertebral region, organ of Zukerkandl, aortocaval region, vas deferens and carotid body; kidneys; and bowel. AACR whole-body MRI surveillance recommendations are in Box 2 [6, 29, 39]. Figure 4 demonstrates paraspinal nodules on whole-body MRI in a girl with hereditary pheochromocytoma and paraganglioma syndrome, confirmed as paragangliomas on resection.

Box 2

Hereditary paraganglioma and pheochromocytoma syndrome

- Neck-to-pelvis whole-body MRI, alternating with
- Chest-to-pelvis whole-body MRI + dedicated neck MRI
- Every 24 months, starting at 6–8 years

Neurofibromatosis type 1

Neurofibromatosis type 1 (NF1; OMIM #162200) is also autosomal-dominant, arising from an *NF1* gene mutation on chromosome 17q. Onset of NF1 is in childhood, with an incidence at birth of between 1/900 and 1/2,800, prevalence of 1/4,150–4,950, and variable penetrance, with 50% of mutations occurring de novo [26, 41, 42]. The clinical criteria defined by the National Institutes of Health (NIH) in 1987 include the occurrence of café au lait macules, intertriginous freckles, cutaneous or plexiform neurofibromas, optic

Fig. 1 Whole-body MRI in a 14-year-old boy with Li–Fraumeni syndrome and left rib osteosarcoma. A series of coronal whole-body short-tau inversion recovery (STIR) images were obtained. **a** The baseline study shows a small focus of high signal from the rib lesion (*arrow*), seen in retrospect. **b** Rib lesion mimics adjacent axillary lymph nodes of similar size, shape and signal (*curved arrow*) in an adjacent slice. **c** One year later, also in retrospect, the lesion (*arrow*) is seen at the site of fusion of two stacks (*arrowheads*). **d** The lesion (*arrow*) has become progressively larger at the time of detection 3 years from baseline. **e, f** Single-station images showing the lesion (arrows) at 3 years (**e**) compared with the baseline (**f**) whole-body MRI

pathway gliomas, bone dysplasia and Lisch nodules [26, 42]. Less reliably manifesting in children younger than 8 years, genetic testing might be warranted if only skin lesions are present, with developmental and neurocognitive impairment accompanying these multisystem lesions [26, 43]. There is less than 1% risk of the following neoplasms (1–2% for central nervous tumors): juvenile myelomonocytic leukemia, embryonal rhabdomyosarcoma (genitourinary more common than orbital), malignant peripheral nerve sheath tumors, optic pathway gliomas, pilocytic astrocytomas, duodenal endocrine tumors and gastrointestinal stromal tumors, and manifold increase in breast cancer in middle age [26, 44, 45].

Anatomical sites of high risk in NF1 warranting careful review on whole-body MRI are the brain, orbits, bone marrow

Fig. 2 Li–Fraumeni syndrome in a 3-year-old boy. **a, b** Coronal whole-body short-tau inversion recovery (STIR) images show (**a**) evidence of a previous right enucleation for an orbital rhabdomyosarcoma (*arrow*) and (**b**) a new right suprarenal mass, confirmed as an adrenocortical carcinoma (*arrowheads*)

and peripheral nerves; and less-frequent sites are the adrenals, urogenital system, bowel, soft tissue/muscle and skin [6]. Although lesions are widespread, unlike Li–Fraumeni syndrome and hereditary pheochromocytoma and paraganglioma syndromes, periodic whole-body MRI surveillance is not advocated because of the low level of malignancy in childhood [26]. Instead, the AACR recommendation is for a single baseline whole-body MRI prior to transition to adulthood if asymptomatic to guide long-term monitoring of malignant peripheral nerve sheath tumors in particular, with clinical optic pathway glioma assessment (Box 3) [6, 26]. Figure 5 demonstrates whole-body MRI in an 11-year-old girl with NF1; applying risk stratification, the left tibial lesion was considered to be of low suspicion, supported by radiographic findings, without evidence of congenital tibial pseudarthrosis [42].

Box 3

Neurofibromatosis type 1

Whole-body MRI baseline scan at 16–20 years of age

Fig. 3 Li–Fraumeni syndrome in a 7-year-old boy. **a–c** Nonspecific bone marrow hyperintensity is evident in the proximal right tibia (*arrows*) on (**a**) coronal whole-body MRI short-tau inversion recovery sequence, (**b**) targeted fat-suppressed axial T2-weighted image, and (**c**) inverted coronal diffusion-weighted image (b=800 mm/s^2). This did not restrict on apparent diffusion coefficient map (not shown). The abnormal signal resolved on a dedicated knee MRI at 1 month later

Neurofibromatosis type 2 and schwannomatosis

Neurofibromatosis type 2 (NF2; OMIM #101000) results from a heterogeneous germline mutation at the *NF2* locus on chromosome 22q, with an incidence of 1/25,000 live

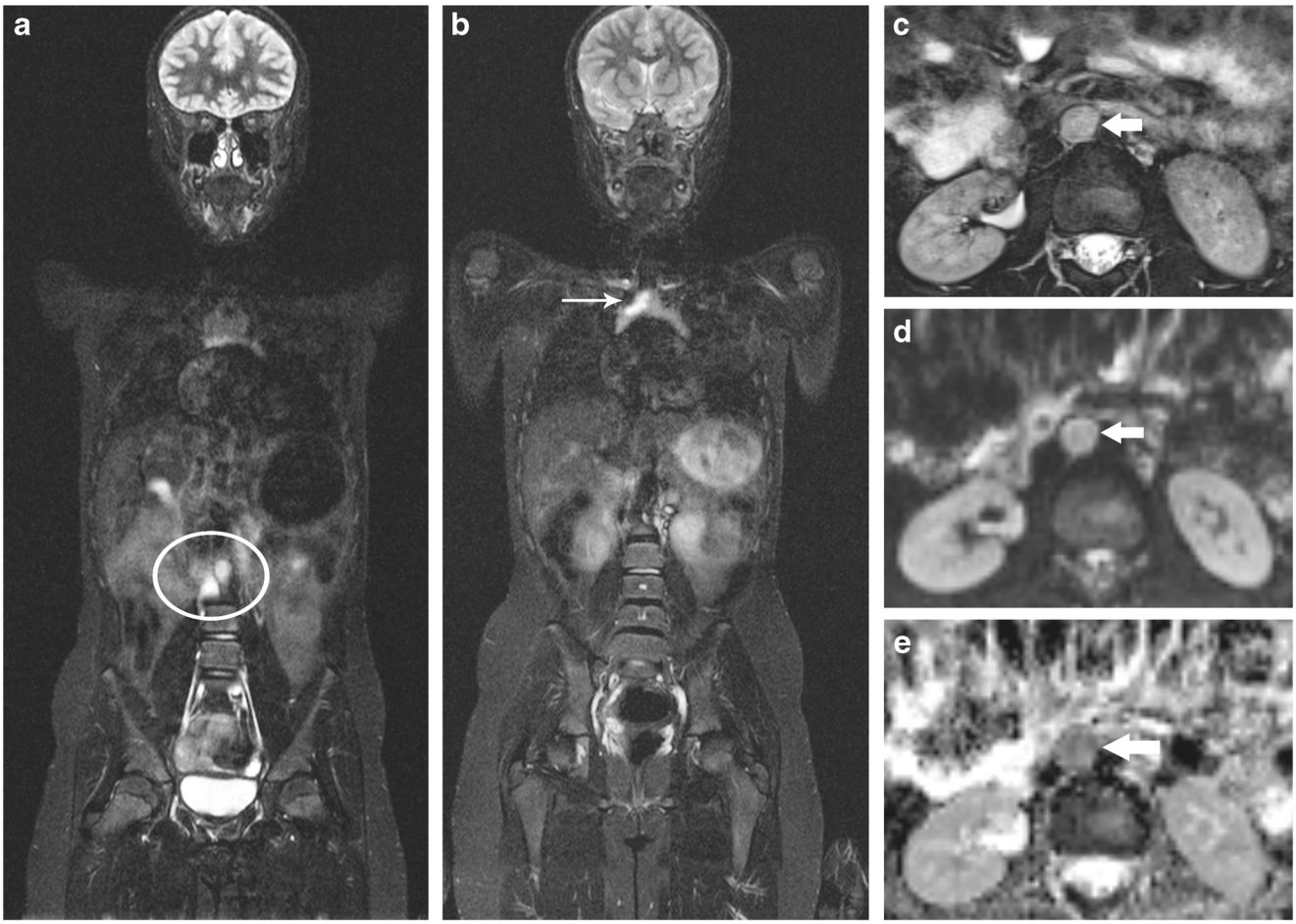

Fig. 4 Hereditary paraganglioma and pheochromocytoma syndrome in a 12-year-old girl. **a, b** Whole-body MRI utilizing coronal short tau inversion recovery (STIR) sequence reveals paraspinal nodules (*oval*) with incidental finding of a thymic cyst (*arrow*). **c–e** Follow-up whole-body MRI (not shown) was supplemented by (**c**) targeted imaging of the retroperitoneum with axial fat-suppressed T2-W, and (**d**) axial diffusion-weighted imaging (b=1,000 s/mm^2) with (**e**) an apparent diffusion coefficient map. This confirmed paraspinal nodules, one retrocaval (*arrows*) showing mild restriction, proved on resection to be paragangliomas

births and almost 100% penetrance by late adulthood [27, 46]. Schwannomatosis (OMIM #162091 and #600574) is a separate entity, with heterogeneous gene mutations affecting *SMARCB1* and *LZTR1* loci on chromosome 22q [27]. Childhood malignancy is rare, with neoplasms usually benign, and includes schwannoma (Fig. 6), meningioma and low-grade ependymoma [27, 44, 46]. Anatomical locations warranting careful review on whole-body MRI include the brain, spine and internal auditory meati, in addition to regional MRI of the internal auditory meati, with AACR surveillance recommendations in Box 4 [6, 27]. As is the case in many cancer predisposition syndromes, the time to stop surveillance imaging has not been clearly established. Although not specific for whole-body MRI, in a 2011 update Evans [47] advocated screening in neurofibromatosis type 2 until the fourth decade, acknowledging the safe time to stop monitoring is unknown.

Box 4

Neurofibromatosis type 2 and schwannomatosis

- Baseline whole-body MRI, timing based on symptoms and at location of symptoms
- Internal auditory meati MRI every 6–24 months (6 months if positive)
- Spine MRI every 24–36 months (6 months if positive)

Hereditary retinoblastoma

Retinoblastoma (OMIM #180200) is the commonest intraocular malignancy, with an incidence in infancy of 1/15,000 [48]. Hereditary retinoblastoma accounts for up to 40% of cases, with an *RB1* germline mutation of one allele on chromosome 13q14.2 de novo occurring more commonly than autosomal-

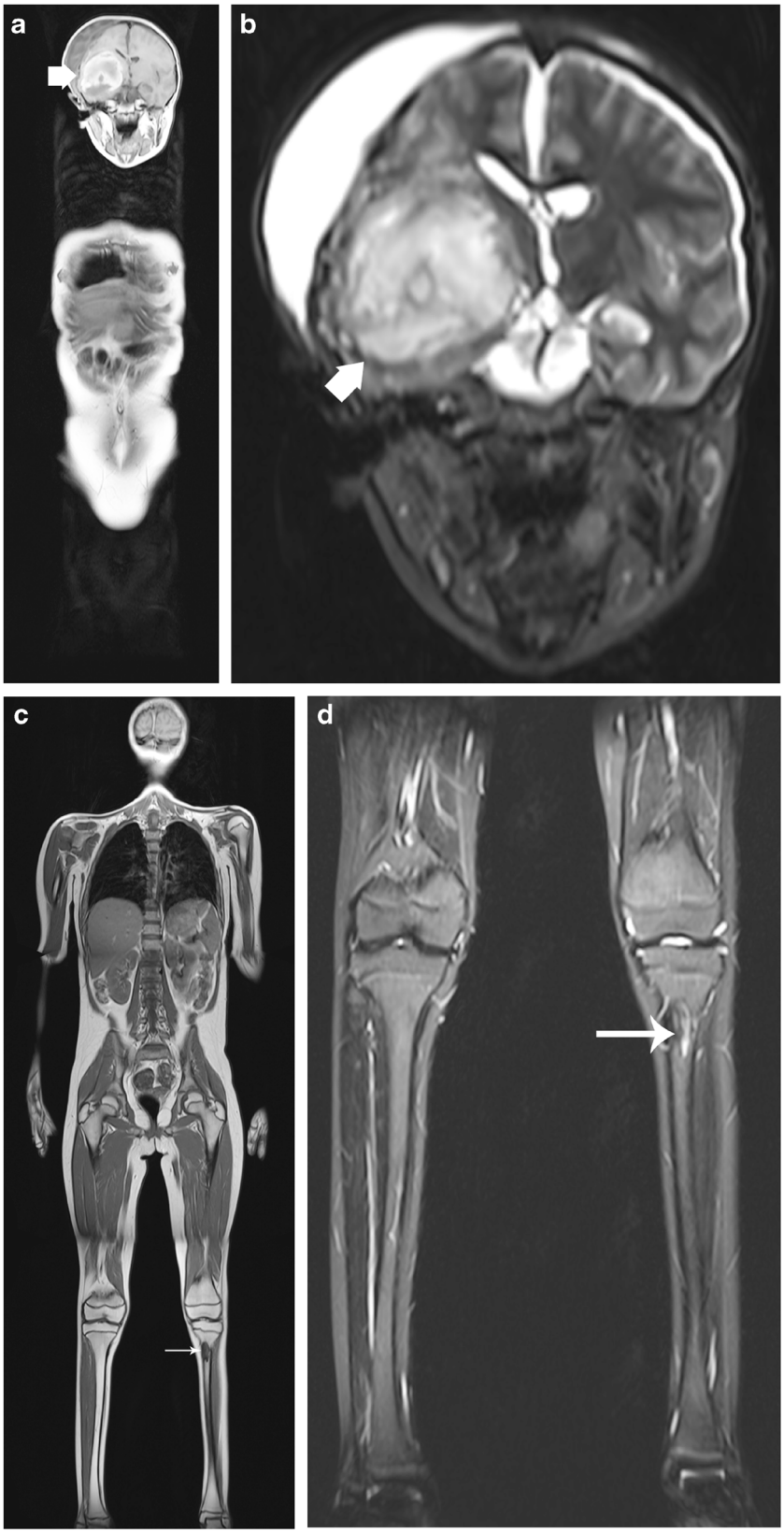

Fig. 5 Neurofibromatosis type 1 in an 11-year-old girl. Coronal whole-body MRI including T1-weighted (**a**, **c**) and short-tau inversion recovery (**b**, **d**) sequences, with single-station images displayed in (**b**) and (**d**). Images (**a**) and (**b**) show a biopsy-proven right temporal sarcoma with a circumscribed temporal lobe lesion (*arrows*), with heterogeneous intermediate to low signal on (**a**), heterogeneous high signal on (**b**), and a large overlying extra-axial fluid collection of low signal on (**a**) and high signal on (**b**). **c**, **d** An intramedullary ovoid lesion is in the proximal left tibia (*arrows*), well-defined and demonstrating low signal on (**c**), and less-defined and demonstrating intermediate to high signal on (**d**), consistent with a non-ossifying fibroma on radiographs (not shown)

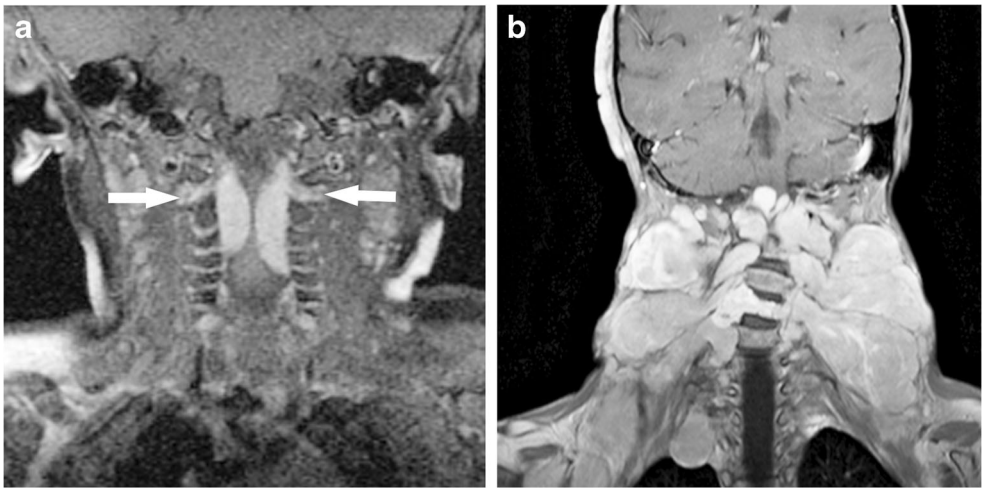

Fig. 6 Neurofibromatosis type 2 with multiple cervicothoracic schwannomas gradually increasing over time, leading to cord compression in an 11-year-old boy. Targeted coronal fat-suppressed T1-weighted post-contrast images of the cervical spine (**a**) on initial imaging at 8 months old show extradural lesions with foraminal extension (*arrows),* and (**b**) 10 years later, exuberant paravertebral masses

dominant inheritance by a factor of 4:1 [28, 48]. Penetrance is 90–95%. Hereditary retinoblastoma is often detected before 1 year of age — especially if bilateral — with 95% diagnosed by 5 years. Three percent to 5% of children with unilateral or bilateral hereditary retinoblastoma also develop a midline primitive neuroectodermal tumor or pineoblastoma early on [28, 49]. Referred to as trilateral retinoblastoma, this has a significantly worse outcome [28, 48, 50].

Survivors of hereditary retinoblastoma face an increased lifetime risk of a second or subsequent malignant neoplasm, contributing to patient mortality as survival for hereditary retinoblastoma reaches greater than 95% [28]. Presenting in different decades throughout life, second malignant neoplasms include osteosarcoma, soft-tissue sarcoma, nasal/orbital tumors, melanoma, and lung, bladder, breast and uterine carcinomas [28, 48, 50]. While noting there is no consensus for whole-body MRI, when it is performed the key anatomical sites for review are the brain, orbits, bones and soft tissue. The AACR whole-body MRI surveillance recommendation is for whole-body MRI to commence slightly later than in other cancer predisposition syndromes, in line with second malignant neoplasm onset, and to avoid general anesthesia (Box 5) [6, 28]. However in some centers, whole-body MRI is performed under general anesthesia in younger patients with retinoblastoma if screening for metastatic disease. As the non-specific bone marrow hyperintensities in Fig. 7 highlight, such findings warrant close monitoring because osteosarcoma is the earliest presenting second malignant neoplasm.

Box 5

Hereditary retinoblastoma

- Whole-body MRI every 12 months from 8 to 10 years
- Brain MRI every 6 months to 5 years

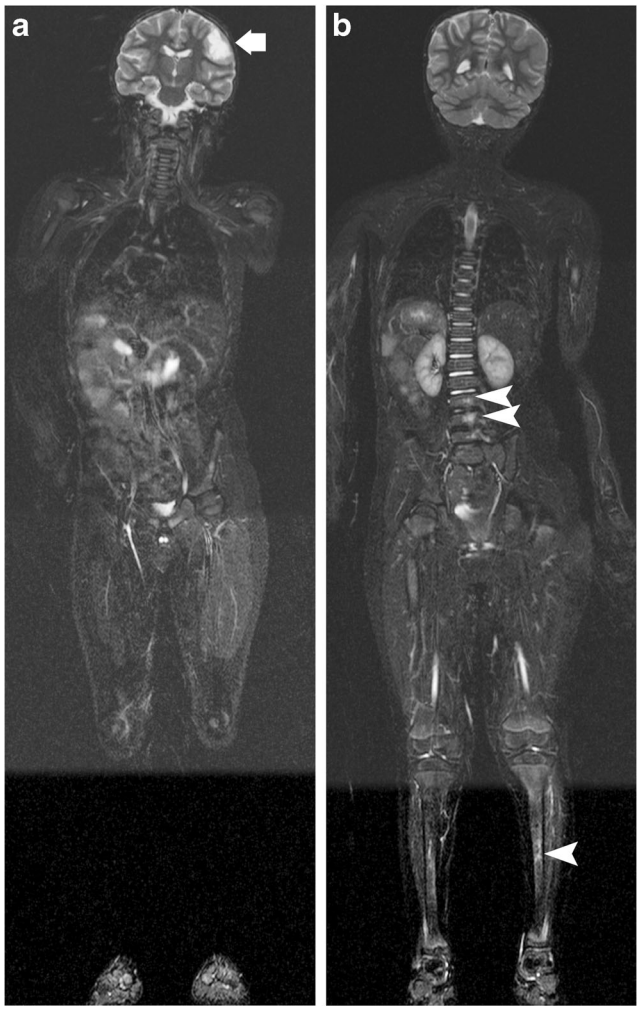

Fig. 7 Hereditary retinoblastoma in a 4-year-old boy. **a, b** Whole-body MRI utilizing coronal short tau inversion recovery (STIR) sequence shows (**a**) increased signal in the left parietal lobe following treatment of a central nervous system metastasis (*arrow*), and (**b**) nonspecific bone marrow STIR hyperintensities in the lumbar vertebrae and left tibia (*arrowheads*)

Fig. 8 Constitutional mismatch repair deficiency in a 17-year-old girl with a history of a colectomy and duodenectomy for adenocarcinoma and astrocytoma. **a** Whole-body MRI utilizing coronal short tau inversion recovery (STIR) sequence demonstrates a complex left renal cyst (*arrow*). **b** The cyst (*arrow*) is better seen on a single-station image, stable when compared with prior imaging but warranting continued close observation. **c** An additional STIR single-station image demonstrates a small simple left paraspinal cyst (*arrowhead*), also stable. The renal cyst (*arrow*) is partially seen

Constitutional mismatch repair deficiency syndrome

Constitutional mismatch repair deficiency syndrome (OMIN #276300) is rare, with an autosomal-recessive pattern of inheritance resulting from biallelic *MMR* germline mutations affecting 1 of 4 genes [51]. However relative tumor risk is high, with a wide tumor spectrum and age of onset, median age for first malignancy being 7.5 years, with core tumors being brain, gastrointestinal and hematologic malignancies [30, 51]. Brain tumors, in particular gliomas, and hematologic malignancies including non-Hodgkin lymphoma, T-cell acute lymphoblastic leukemia and acute myeloid leukemia occur earliest, with brain tumors commonest [51]. Colorectal and small-bowel carcinomas, small-bowel adenomas and genitourinary neoplasms, osteosarcoma, rhabdomyosarcoma and pilomatricoma occur later, with a specific scoring system also capturing these and other clinical features very sensitive for diagnosis [30, 51]. A number of the genes in constitutional mismatch repair deficiency syndrome overlap with Lynch syndrome, autosomal-dominant and manifesting in the fourth decade primarily with hereditary non-polyposis colorectal and other tumors, and a Lynch-syndrome-associated tumor in a relative is one criterion in diagnosing constitutional mismatch repair deficiency syndrome [51].

Brain, bowel and bone marrow are key anatomical sites on whole-body MRI review, followed by skin, soft tissue and muscle [6]. Lynch syndrome also involves the brain and bowel, with increased involvement in the kidneys, urinary bladder, uterus and ovaries. AACR surveillance recommendations are in Box 6 [6, 30]. Figure 8 demonstrates the tumor spectrum in a 17-year-old girl with constitutional mismatch repair deficiency syndrome who had extensive bowel resection and treatment for astrocytoma, with stable renal and paraspinal lesions under review.

Box 6

Constitutional mismatch repair deficiency syndrome (and Lynch syndrome)

- Whole-body MRI every 12 months from 6 to 8 years (when not needing general anesthesia)
- Brain MRI every 6 months from diagnosis
- Abdominal and pelvic ultrasound every 6 months from 1 year

Standardized reporting

Structured reporting can range from the use of templates to standardized reporting systems. In cancer predisposition syndromes, they can facilitate systematic review, further optimizing whole-body MRI interpretation, and can be particularly beneficial where serial imaging is undertaken as in whole-body MRI surveillance. This can help emphasize suspicious lesions for follow-up, aid in comparison with prior studies for more inexperienced readers, and improve report clarity for patients moving among institutions for their investigations and management [6, 18].

Conclusion

Surveillance imaging in childhood cancer predisposition syndromes needs to be guided by the balance of risks and benefits, with harmonization of surveillance and diagnostic imaging pathways. For whole-body MRI, optimizing image interpretation through knowledge of the tumor spectrum and sites for particular syndromes, and a systematic approach, can improve lesion detection, reduce false-positive findings and contribute to improved patient outcomes.

Compliance with ethical standards

Conflicts of interest None

References

1. American Society of Clinical Oncology (2003) American Society of Clinical Oncology policy statement update: genetic testing for cancer susceptibility. J Clin Oncol 21:2397–2406
2. Monsalve J, Kapur J, Malkin D et al (2011) Imaging of cancer predisposition syndromes in children. Radiographics 31:263–280
3. van Engelen K, Villani A, Wasserman JD et al (2017) DICER1 syndrome: approach to testing and management at a large pediatric tertiary care center. Pediatr Blood Cancer 65(1)
4. Druker H, Zelley K, McGee RB et al (2017) Genetic counselor recommendations for cancer predisposition evaluation and surveillance in the pediatric oncology patient. Clin Cancer Res 23:e91–e97
5. Jongmans MC, Loeffen JL, Waanders E et al (2016) Recognition of genetic predisposition in pediatric cancer patients: an easy-to-use selection tool. Eur J Med Genet 59:116–125
6. Greer MC, Voss SD, States LJ (2017) Pediatric cancer predisposition imaging: focus on whole-body MRI. Clin Cancer Res 23:e6–e13
7. Villani A, Tabori U, Schiffman J et al (2011) Biochemical and imaging surveillance in germline TP53 mutation carriers with li-Fraumeni syndrome: a prospective observational study. Lancet Oncol 12:559–567
8. Villani A, Shore A, Wasserman JD et al (2016) Biochemical and imaging surveillance in germline TP53 mutation carriers with li-Fraumeni syndrome: 11 year follow-up of a prospective observational study. Lancet Oncol 17:1295–1305
9. McNeil DE, Brown M, Ching A et al (2001) Screening for Wilms tumor and hepatoblastoma in children with Beckwith-Wiedemann syndromes: a cost-effective model. Med Pediatr Oncol 37:349–356
10. Friedman DN, Lis E, Sklar CA et al (2014) Whole-body magnetic resonance imaging (WB-MRI) as surveillance for subsequent malignancies in survivors of hereditary retinoblastoma: a pilot study. Pediatr Blood Cancer 61:1440–1444
11. Zhang J, Walsh MF, Wu G et al (2015) Germline mutations in predisposition genes in pediatric cancer. N Engl J Med 373:2336–2346
12. Brodeur GM, Nichols KE, Plon SE et al (2017) Pediatric cancer predisposition and surveillance: an overview, and a tribute to Alfred G. Knudson Jr. Clin Cancer Res 23:e1–e5
13. Foulkes WD, Kamihara J, Evans DGR et al (2017) Cancer surveillance in Gorlin syndrome and rhabdoid tumor predisposition syndrome. Clin Cancer Res 23:e62–e67
14. Bueno MT, Martinez-Rios C, la Puente Gregorio A et al (2017) Pediatric imaging in DICER1 syndrome. Pediatr Radiol 47:1292–1301
15. Brenner DJ, Shuryak I, Einstein AJ (2011) Impact of reduced patient life expectancy on potential cancer risks from radiologic imaging. Radiology 261:193–198
16. Mathews JD, Forsythe AV, Brady Z et al (2013) Cancer risk in 680,000 people exposed to computed tomography scans in childhood or adolescence: data linkage study of 11 million Australians. BMJ 346:f2360
17. Kratz CP, Achatz MI, Brugieres L et al (2017) Cancer screening recommendations for individuals with li-Fraumeni syndrome. Clin Cancer Res 23:e38–e45
18. Anupindi SA, Bedoya MA, Lindell RB et al (2015) Diagnostic performance of whole-body MRI as a tool for cancer screening in children with genetic cancer-predisposing conditions. AJR Am J Roentgenol 205:400–408
19. Teixeira SR, Elias Junior J, Nogueira-Barbosa MH et al (2015) Whole-body magnetic resonance imaging in children: state of the art. Radiol Bras 48:111–120
20. Guimaraes MD, Noschang J, Teixeira SR et al (2017) Whole-body MRI in pediatric patients with cancer. Cancer Imaging 17:6
21. Lecouvet FE (2016) Whole-body MR imaging: musculoskeletal applications. Radiology 279:345–365
22. Anupindi SA, Chauvin NA, Nichols KE (2016) Reply to 'Whole-body MRI screening in children with li-Fraumeni and other cancer-predisposition syndromes. AJR Am J Roentgenol 206:W53
23. Tijerin Bueno M, Malkin D, Villani A, Moineddin R (2015) Whole body MRI in children with cancer predisposition syndromes. Pediatr Radiol 45:71
24. Davidson AJ, Disma N, de Graaff JC et al (2016) Neurodevelopmental outcome at 2 years of age after general anaesthesia and awake-regional anaesthesia in infancy (GAS): an international multicentre, randomised controlled trial. Lancet 387:239–250
25. Sadowski EA, Bennett LK, Chan MR et al (2007) Nephrogenic systemic fibrosis: risk factors and incidence estimation. Radiology 243:148–157

26. Evans DGR, Salvador H, Chang VY et al (2017) Cancer and central nervous system tumor surveillance in pediatric neurofibromatosis 1. Clin Cancer Res 23:e46–e53
27. Evans DGR, Salvador H, Chang VY et al (2017) Cancer and central nervous system tumor surveillance in pediatric neurofibromatosis 2 and related disorders. Clin Cancer Res 23:e54–e61
28. Kamihara J, Bourdeaut F, Foulkes WD et al (2017) Retinoblastoma and neuroblastoma predisposition and surveillance. Clin Cancer Res 23:e98–e106
29. Rednam SP, Erez A, Druker H et al (2017) Von Hippel-Lindau and hereditary pheochromocytoma/paraganglioma syndromes: clinical features, genetics, and surveillance recommendations in childhood. Clin Cancer Res 23:e68–e75
30. Tabori U, Hansford JR, Achatz MI et al (2017) Clinical management and tumor surveillance recommendations of inherited mismatch repair deficiency in childhood. Clin Cancer Res 23:e32–e37
31. Schultz KAP, Rednam SP, Kamihara J et al (2017) PTEN, DICER1, FH, and their associated tumor susceptibility syndromes: clinical features, genetics, and surveillance recommendations in childhood. Clin Cancer Res 23:e76–e82
32. Walsh MF, Chang VY, Kohlmann WK et al (2017) Recommendations for childhood cancer screening and surveillance in DNA repair disorders. Clin Cancer Res 23:e23–e31
33. Mehollin-Ray AR, Kozinetz CA, Schlesinger AE et al (2008) Radiographic abnormalities in Rothmund-Thomson syndrome and genotype-phenotype correlation with RECQL4 mutation status. AJR Am J Roentgenol 191:W62–W66
34. Ballinger ML, Ferris NJ, Moodie K et al (2017) Surveillance in germline TP53 mutation carriers utilizing whole-body magnetic resonance imaging. JAMA Oncol 3:1735–1736
35. Ballinger ML, Best A, Mai PL et al (2017) Baseline surveillance in Li-Fraumeni syndrome using whole-body magnetic resonance imaging: a meta-analysis. JAMA Oncol 3:1634–1639
36. Garritano S, Gemignani F, Palmero EI et al (2010) Detailed haplotype analysis at the TP53 locus in p.R337H mutation carriers in the population of southern Brazil: evidence for a founder effect. Hum Mutat 31:143–150
37. Ricketts CJ, Forman JR, Rattenberry E et al (2010) Tumor risks and genotype-phenotype-proteotype analysis in 358 patients with germline mutations in SDHB and SDHD. Hum Mutat 31:41–51
38. Assadipour Y, Sadowski SM, Alimchandani M et al (2017) SDHB mutation status and tumor size but not tumor grade are important predictors of clinical outcome in pheochromocytoma and abdominal paraganglioma. Surgery 161:230–239
39. Jasperson KW, Kohlmann W, Gammon A et al (2014) Role of rapid sequence whole-body MRI screening in SDH-associated hereditary paraganglioma families. Familial Cancer 13:257–265
40. Ricketts CJ, Shuch B, Vocke CD et al (2012) Succinate dehydrogenase kidney cancer: an aggressive example of the Warburg effect in cancer. J Urol 188:2063–2071
41. Evans DG, Howard E, Giblin C et al (2010) Birth incidence and prevalence of tumor-prone syndromes: estimates from a UK family genetic register service. Am J Med Genet A 152A:327–332
42. Van Royen K, Brems H, Legius E et al (2016) Prevalence of neurofibromatosis type 1 in congenital pseudarthrosis of the tibia. Eur J Pediatr 175:1193–1198
43. DeBella K, Szudek J, Friedman JM (2000) Use of the national institutes of health criteria for diagnosis of neurofibromatosis 1 in children. Pediatrics 105:608–614
44. Ahlawat S, Fayad LM, Khan MS et al (2016) Current whole-body MRI applications in the neurofibromatoses: NF1, NF2, and schwannomatosis. Neurology 87:S31–S39
45. Boyd KP, Korf BR, Theos A (2009) Neurofibromatosis type 1. J Am Acad Dermatol 61:1–14
46. Asthagiri AR, Parry DM, Butman JA et al (2009) Neurofibromatosis type 2. Lancet 373:1974–1986
47. Evans DG (2011) Neurofibromatosis 2. In: Adam MP, Ardinger HH, Pagon RA et al (eds) GeneReviews®. University of Washington, Seattle
48. Yamanaka R, Hayano A, Takashima Y (2017) Trilateral retinoblastoma: a systematic review of 211 cases. Neurosurg Rev. https://doi.org/10.1007/s10143-017-0890-4
49. de Jong MC, Kors WA, de Graaf P et al (2014) Trilateral retinoblastoma: a systematic review and meta-analysis. Lancet Oncol 15:1157–1167
50. Dimaras H, Heon E, Doyle J et al (2011) Multifaceted chemotherapy for trilateral retinoblastoma. Arch Ophthalmol 129:362–365
51. Wimmer K, Kratz CP, Vasen HF et al (2014) Diagnostic criteria for constitutional mismatch repair deficiency syndrome: suggestions of the European consortium 'care for CMMRD' (C4CMMRD). J Med Genet 51:355–365